Journal of Physics D: Applied Physics

Collective and cooperative dynamics in transition domains of amorphous polymers with multi-shape memory effect

To cite this article before publication: Xiaodong Wang *et al* 2019 *J. Phys. D: Appl. Phys.* in press https://doi.org/10.1088/1361-6463/ab57d6

Collective and cooperative dynamics in transition domains of amorphous polymers with multi-shape memory effect

Xiaodong Wang[1], Haibao Lu[1,3], Yong Qing Fu[2], Jinsong Leng[1] and Shanyi Du[1]

[1]Science and Technology on Advanced Composites in Special Environments Laboratory, Harbin Institute of Technology, Harbin 150080, China

[2]Faculty of Engineering and Environment, University of Northumbria, Newcastle upon Tyne, NE1 8ST, UK

[3]luhb@hit.edu.cn

Abstract: Multi-shape memory effect (multi-SME) in amorphous shape memory polymers (SMPs) linked with collective and cooperative rearrangements and accommodations of monomeric segments, thus leading to generation of complex thermodynamic modes. In this study, an extended domain size model is initially formulated to describe various temperature-dependent relaxation behaviors and domain transitions in amorphous SMPs. According to the Adam-Gibbs theory, a cooperative model is employed to identify the principle role of domain size in the collective dynamics of multi-SME in amorphous SMPs. The phase transition theory is then combined with multi-branch Kelvin model to describe the collective and cooperative relaxation behaviors of the SMPs with multiple transition domains. It is shown that the proposed model is able to characterize the thermomechanical transitions and multiple shape recovery processes. Finally, the model is applied to predict shape recovery behavior of SMPs with triple- and quadruple-SME,

respectively, and the theoretical results are well validated by the experimental ones.

Keywords: shape memory polymer, multi-shape memory effect, Adam-Gibbs theory, cooperative domain model

1. Introduction

Shape memory polymers (SMPs) are one type of smart materials that can recover to their permanent shapes [1,2] from a pre-deformed temporary shape upon external stimuli such as Joule heating, infrared-light radiation, laser heating and solvent [3-7]. Among these, thermal actuation of SMPs is the most popular approach to trigger the shape recovery and has been widely used in smart textiles [8], intelligent medical devices [9], sensor and actuators [10], self-deployable and self-folding structures in spacecraft [11,12], as well as aerospace applications [13]. Therefore, the thermodynamics of SMPs have been identified as one of the critical issues to explore the working mechanism of shape memory effect (SME) and extend the potential applications of SMPs. According to literature [14,15], a conventional SMP can only memorize one temporary shape in each shape memory cycle, whereas new types of SMPs have been synthesized recently to show multi-SME, which enables the polymers to memorize more than two temporary shapes [16-21]. Multiple and reversible transitions of various phases with well-separated glass transition zones have been identified as the driving force for the multi-SME in SMPs [18,22]. Digital manufacturing technologies have also been used to control the shape changing sequence of SMPs and exploit their multi-SME [23,24].

To theoretically explore the physics and mechanics of SMPs with multi-SMEs, a model of their segmental relaxation behavior was initially proposed by Yu et al based on the generalized Maxwell model [25]. The multiple phase transitions were formulated based on the thermodynamics of structural configurations [26] and the proposed models well predicted the multiple shape recovery behaviors of the SMPs [27-29]. However, as is well known, thermomechanical properties of the SMPs are resulted from the cooperative rearrangement of all segments inside, and the cooperative and collective dynamics have never been considered during the studies of the multi-SMEs of the SMPs.

In this study, we firstly formulate a cooperatively rearranging domain model to characterize the multi-SME, according to the Adam and Gibbs theory [30-33]. Different from the existing modeling approaches that are mainly replied on the thermo-viscoelastic theory [22,25], this model provides an effective approach to investigate the multi-SMEs based on the physical parameters such as activation energy and cooperative domain size. The phase transition theory is then combined with a multi-branch relaxation model to describe the collective and cooperative rearrangement of monomeric segments. Results show that the proposed model is able to characterize and predict the thermomechanical responses and describe the shape recovery processes. The proposed model is then applied to predict the shape memory behavior of SMPs with triple- and quadruple-SMEs, respectively, and theoretical analysis results have been validated using the experimental ones. It should be noted that this article mainly is focused on the multiple phase transition and multi-SME of

amorphous SMPs, which undergo glass transitions to achieve their shape deformation and recovery.

2. Cooperative dynamics of the SME in SMP

As discussed in the previous studies [34,35], the SME in amorphous polymers is resulted from the glass transition where the frozen segments are changed into active ones and the stored mechanical strain is released. Here we use a cooperative domain model to characterize the temperature dependences of configurable entropy and relaxation behavior in the shape recovery process [30,31]. In this model, the conformer (e.g., the smallest segmental unit of rotation) is surrounded by other conformers. If the conformer is able to undergo relaxation, its neighbors must also move in a cooperation way [30]. The domain size (z) is defined as the number of conformers which are meshed with each other and relaxed simultaneously during the relaxation process [31-33]. With an increase in temperature, the domain size decreases and the mobility of polymer segment is significantly increased.

For one mole of conformers in polymer, there are N_z domains consisting of z numbers of conformers. Therefore, the domain size could be written as follows [32]:

$$z = N_A / N_z \tag{1}$$

where N_A is the Avogadro constant.

The conformational entropy S_c for one mole of conformers with N_z domains is [32]:

$$S_c = N_z k_B \ln \Omega \tag{2}$$

where k_B is the Boltzmann constant, and Ω is the number of states that a conformer can have.

According to the Adam-Gibbs theory [30], parameter S^* is defined as the maximum value of conformational entropy (S_c) when all the conformers are relaxed independently at the high-temperature limit of T^*. According to this definition, when $S_c = S^*$ at the temperature of T^*, the domain size (z) equals to 1. Based on equation (2), parameter S^* can be written as [33]:

$$S^* = N_A k_B \ln \Omega \tag{3}$$

Assuming that free energy, enthalpy, and entropy are all scaled proportionately [32], then we can obtain:

$$S_c / S^* = \frac{T^*}{T^* - T_0} \cdot \frac{T - T_0}{T} \tag{4}$$

where there is no cooperativity among the conformers at the high-temperature limit T^*. On the other hand, all conformers are meshed with each other and cooperatively relaxed at the low-temperature limit T_0 simultaneously.

By substituting equations (2), (3) and (4) into equation (1), the domain size z can be expressed as:

$$z = N_A k_B \ln c_1 / N_z k_B \ln c_1 = S^* / S_c = \frac{T}{T - T_0} \cdot \frac{T^* - T_0}{T^*} \tag{5}$$

As is discussed above [34,35], the SME in SMP is originated from the transition of the monomeric segments from a frozen phase into an active one [15,35]. On the other hand, the conformer in the same cooperative domain are relaxed simultaneously [31-33]. Therefore, the energy barrier for a domain to relax is determined by the

energy barriers of all the conformers inside the SMP [32]. Here the activation energy (ΔH) for a domain to relax can be written as:

$$\Delta H = z\Delta\mu = \frac{T}{T - T_0} \cdot \frac{T^* - T_0}{T^*} \Delta\mu \tag{6}$$

where $\Delta\mu$ is the activation energy of a single conformer to relax independently.

The relaxation time (λ), one of the most critical parameters to determine the viscoelastic behavior of SMPs, can be derived from the domain size and temperature as follows [32]:

$$\lambda = \lambda_r \exp\left(\frac{\Delta\mu}{R}\left(\frac{z}{T} - \frac{z_r}{T_r}\right)\right) \tag{7}$$

where R=8.314 $J/(mol \cdot K)$ is the gas constant, λ_r and z_r are the relaxation time and domain size at the referenced temperature of T_r, respectively.

According to the equations (6) and (7), the relaxation behavior can be studied by means of domain size model for the amorphous SMPs.

3. Constitutive relationships and collective dynamics

3.1 Constitutive relationships of multi-SME in SMP

The multi-SME was firstly discovered in the Nafion based SMP, which is originated from the broadened glass transition temperature region from 55°C to 140°C [19]. According to the domain size model, multi-SME is resulted from the various relaxation processes during the glass transition process. Here the relaxation process is governed by the relaxation equation, e.g., equation (7). However, each relaxation process is controlled by its domain size (z), and the conformers in the same domain

are assumed to have the same relaxation time and relax, simultaneously. Therefore, the multi-SME is originated from the collective dynamics of various relaxation processes in the SMP. Figure 1 presents a schematic illustration of the relaxation behaviors in the Nafion SMP by a discrete domain size.

Meanwhile, an extended Kelvin model [25] is introduced to characterize the relaxation and viscoelastic behavior of each domain which is composed of one frozen phase and one active phase. Here, the frozen phase presents an elastic behavior, whereas the active one presents a viscoelastic behavior. Thus, we have,

$$\sum_{i=1} \phi_f(z_i) + \sum_{i=1} \phi_a(z_i) = 1 \tag{8}$$

where $\phi_f(z_i)$ and $\phi_a(z_i)$ are the volume fractions of the frozen and active phases, respectively, in the domain with the domain size z_i.

[Figure 1]

According to the phase transition theory [34], temperature dependent volume fraction of the frozen phase ($\phi_f(T)$) equals to the ratio of stored strain (ε_s) and pre-stretched strain (ε_{pre}), therefore,

$$\varepsilon_s(T) = \phi_f(T) \cdot \varepsilon_{pre} \tag{9}$$

As discussed above, the SMP contains *n* number of domains, of which one domain has one frozen phase. Therefore, the average volume fraction of the frozen phase can be written as,

$$\phi_f(T) = \sum_{i=1}^{n} \left(\phi_f(z_i) \cdot z_i / \sum_{i=1}^{n} z_i \right) \tag{10}$$

where superscript *i* represents the *i*th relaxation domain, and the term $z_i / \sum_{i=1}^{n} z_i$ is

used to represent the volume fraction of the *i*th domain in the SMP.

According to the transition state theory [35-37], $\phi_f(z_i)$ is a function of both temperature T and time t:

$$\phi_f(z_i) = \left[1 - \exp(-\Delta H(z_i)/RT)\right]^{\frac{t}{\tau_{0i}}} \tag{11}$$

where τ_{0i} is initial relaxation time which is a constant.

Substituting equation (6) into (11), we can obtain:

$$\phi_f(z_i) = \left[1 - \exp\left(-\frac{z_i \Delta\mu}{RT}\right)\right]^{\frac{t}{\tau_{0i}}} \tag{12}$$

In combination of equations (9), (10) and (12), we can obtain an expression of the stored strain in the SMP as functions of both temperature T and time t,

$$\varepsilon_s = \sum_{i=1}^{n}\left(\left[1 - \exp\left(-\frac{z_i \Delta\mu}{RT}\right)\right]^{\frac{t}{\tau_{0i}}} \cdot z_i / \sum_{i=1}^{n} z_i\right) \cdot \varepsilon_{pre} \tag{13}$$

Under the continuous heating, polymer can obtain an average domain size of ($\bar{z}$) [27], therefore, equation (13) can be rewritten as,

$$\varepsilon_s = \left[1 - \exp\left(-\frac{\bar{z}\,\Delta\mu}{RT}\right)\right]^{\frac{t}{\bar{\tau}_0}} \cdot \varepsilon_{pre} \tag{14}$$

Here, modeling results obtained using equations (13) and (14) are plotted to compare with the experimental data reported in reference [19] for the Nafion SMP. Results show a dual-SME and multi-SME induced by heating. In this section, the Universal Global Algorithm (UGO) method is adopted here in order to determine the values of all the parameters used in equations (13) and (14), which are listed in Table 1.

The modeling results of Equation (14) are further used to compare with the

experimental data of the Nafion SMP with a dual-SME. As shown in Figure 2(a), Nafion SMP shows an SME and presents a continuous changes of strains when the temperature is increased from 293 K to 413 K at a heating rate of $q = 4.5 K/\min$. With an increase of temperature, the pre-stored strain is gradually released and decreased from 43.64% to 0.99%. Clearly the modeling results shown in Figure 2(a) are well fit with the experimental results.

[Table 1]

On the other hand, this Nafion SMP also presents a multi-SME phenomenon using a segmental heating process as shown in Figure 2(b). Both time and temperature will significantly influence this multi-SME. At this condition, domains with different sizes have different hysteresis patterns upon the release of the stored strain. The complex form of equation (13) is used to compare with the experimental data of the Nafion SMP. Five transition processes have been presented during the strain recovery process, when the SMP undergoes five isothermal heating processes, i.e., (1) from 10min to 47.5 min at a temperature of 240 K; (2) from 52.5 min to 92 min at a temperature of 263 K; (3) from 97 min to 135 min at a temperature of 300 K; (4) from 140 min to 178.5 min at a temperature of 330 K and (5) from 183.5 min to 224.5 min at a temperature of 360 K. The modeling results shown in Figure 2(b) reveal that the domain size is critically determined by the temperature, as presented in equation (5). Meanwhile, the relaxation behavior of the SMP is also critically determined by the domain size. Therefore, five relaxation behaviors have been observed due to the various holding temperatures of $T_0(K)$=240 K, 263 K, 300 K, 330 K and 390 K.

[Figure 2]

Effect of segmental heating procedures on the thermomechanical properties (especially the multi-SME) of the SMP is further investigated. As shown in Figure 1, different relaxation domains are in series connections. Therefore, the modulus of the SMP can be obtained,

$$E(T) = \phi_f(T)E_f + \phi_a(T)E_a \tag{15}$$

where E_f and E_a are the moduli of the frozen and active phases, respectively.

The modulus of the frozen phase can be obtained using the following phenomenological equation [38],

$$\log E_f(T) = \log E(T^{ref}) - a(T - T^{ref}) \tag{16}$$

where $E(T^{ref})$ is the Young's modulus, T^{ref} is the referenced temperature and a is a constant parameter linking with the temperature sensitivity of the material.

The modeling results obtained using the equation (15) as shown in Figure 3 are further plotted to compare with the experimental data measured using dynamic mechanical analysis (DMA) for the Nafion SMP, reported in reference [19]. Values of the parameters used in equation (16) are listed in Table 1. It is revealed that the storage moduli of the SMP are gradually decreased from 900 MPa to 2.2 MPa with the temperature increased from 293 K to 420K, and the changes of the storage moduli prove that the Nafion SMPs show a dual-SME at a constant heating rate. The modeling results of the storage moduli are in well agreements with the experimental results. Therefore, the proposed model can be used to characterize and predict the changes of storage moduli and thermomechanical properties of the Nafion SMP.

[Figure 3]

When an external force σ_0 is applied, the overall strain ($\varepsilon(i)$) of SMP is divided into three parts, which can be expressed as:

$$\varepsilon(i) = \varepsilon_{frozen}(z_i) + \varepsilon_{dashpot}(z_i) + \varepsilon_{spring}(z_i) \tag{17}$$

where $\varepsilon_{frozen}(z_i)$, $\varepsilon_{dashpot}(z_i)$, $\varepsilon_{spring}(z_i)$ are the strains of frozen phase, dashpot and spring in active phase in the *i*th domain, respectively, as shown in Figure 1.

According to the Voigt model [39,40], the function of $\varepsilon_{dashpot}(z_i)$ with respect to time *t* is given by:

$$\varepsilon_{dashpot}(z_i) = \varepsilon(\infty)(1-e^{-t/\tau}) \quad (\varepsilon(\infty) = \sigma_0 / E_2) \tag{18}$$

where $\varepsilon(\infty)$ is the equilibrium strain when the time reaches to infinite, E_2 is the modulus of the spring and τ is the decayed time.

When the temperature is decreased from T_1 to T_2, the active phases are gradually transformed into their frozen states, and the strain $\varepsilon_{dashpot}(z_i)$ is therefore decreased. The time-dependent $\varepsilon_{dashpot}(z_i)$ can be expressed as:

$$\frac{d\varepsilon_{dashpot}(z_i)}{ds} = \frac{\varepsilon(\infty)}{\tau} e^{-s/\tau} \tag{19}$$

where s is the time. With decrease in the temperature, the $\varepsilon_{dashpot}$ can be written as:

$$\varepsilon_{dashpot} = \sum_{i=1}^{n} \left\{ \int_0^t \left[\frac{\varepsilon_\infty}{\tau} e^{-s/\tau} \phi_a(z_i)\Big|_{T=T_1-qs} z_i / \sum_{i=1}^{n} z_i \right] ds \right\} \tag{20}$$

where q is the heating/cooling rate.

The moduli of the frozen and active phases in different domains are the same due to the same molecular structure, thus, the $\varepsilon_{frozen}(z_i)$ and $\varepsilon_{spring}(z_i)$ can be expressed using the following equations:

$$\varepsilon_{frozen} = \sum_{i=1}^{n} \varepsilon_{frozen}(z_i) = \frac{\sigma_0}{E_f}\phi_f(T); \quad \varepsilon_{spring} = \sum_{i=1}^{n} \varepsilon_{spring}(z_i) = \frac{\sigma_0}{E_1}\phi_a(T) \tag{21}$$

By substituting equations (20) and (21) into equation (17), the overall strain ($\varepsilon_{mechanic}$) caused by the external mechanical force can be written using:

$$\varepsilon_{mechanic} = \frac{\sigma_0}{E_f}\phi_f(T) + \sum_{i=1}^{n}\int_0^t \left[\frac{\varepsilon_\infty}{\tau} e^{-s/\tau} \phi_a(z_i)\Big|_{T=T_1-qs} z(i) / \sum_{i=1}^{n} z(i) \right] ds + \frac{\sigma_0}{E_r}\phi_a(T) \tag{22}$$

On the other hand, the instant strain ($\varepsilon_{\text{instant}}$) will disappear at a temperature of T_2, which can be described using,

$$\varepsilon_{\text{instant}} = \frac{\sigma_0}{E_f}\phi_f\Big|_{T=T_2} + \varepsilon_{spring}(z_i)\phi_a\Big|_{T=T_2} = \frac{\sigma_0}{E_f}\phi_f\Big|_{T=T_2} + \frac{\sigma_0}{E_r}\phi_a\Big|_{T=T_1}\phi_a\Big|_{T=T_2} \tag{23}$$

While the decayed strain ($\varepsilon_{decayed}$) can be obtained using the following equation:

$$\varepsilon_{decayed} = \varepsilon_{dashpot}\phi_a\Big|_{T=T_2} \exp(-t/\tau\Big|_{T=T_2}) \tag{24}$$

Therefore, the stored strain (ε_{store}) can be obtained by combining equations (22), (23) and (24):

$$\varepsilon_{store} = \varepsilon_{mechanic} - \varepsilon_{\text{instant}} - \varepsilon_{decayed} \tag{25}$$

Figure 4 shows the numerical results of the strain and stress as a function of time at the differently controlled cooling and heating rates. The experimental data of the Nafion SMP reported in reference [19] are used here to compare with our modeling results. Table 1 lists the fit data, and E_1 =1.02MPa and E_2 =1.21MPa. These parameters are used to determine the relaxation time and the volume fraction of frozen phase (ϕ_f) at the specific loading temperature, and then they are substituted into equations (22), (23) and (24)."

As revealed from the modeling results, the stored strain (ε_{store}) of SMP is gradually increased from 0% to 50% when the temperature is decreased from 413 *K* to 326 *K* at

a constant cooling rate. It is then relaxed to 40% from 50% at the temperature of 326 *K* within the relaxation time from 28 min to 36.3 min, when the external force is not applied to the SMP. Afterwards, a larger external stress is then applied on the SMP, of which the stored strain (ε_{store}) is increased from 40% to 105%. After this stage, the free relaxation behavior of SMP is only determined by temperature and heating rate, and results showed that there is no external stress applied on it during the relaxation time from 63.8 min to 128 min. During the free relaxation (recovery) stage, the stored strain (ε_{store}) in SMP is gradually released. A two-step recovery process has been obtained as shown in Figure 4 which is resulted from a two-step heating processes, e.g., one is from 293 *K* to 326 *K*, whereas the other is from 326 *K* to 413 *K*. Clearly the modeling results obtained using the equation (25) fit well with experimental data [19] of the Nafion SMP with the multi-SMEs.

[Figure 4]

3.2 Collective dynamics of multi-SME in SMP

The other approach for SMPs to achieve multi-SMEs is to generate two or more temporarily phases in the SMP, i.e., each phase shows inherent relaxation and shape recovery behavior [16,18]. To formulate a constitutive relationship of the SMP with multiple transition domains, the relaxation behavior of the SMPs is assumed to be resulted from the cooperative and collective dynamics of all the domains, as illustrated in Figure 5. Each domain represents a temporarily phase, which is incorporated of a hard phase and an active one, and their relaxation behavior is ruled

by the extended Maxwell model.

[Figure 5]

According to the Takayanagi principle [41] and equation (15), the storage modulus ($E(T)$) of the SMP can be calculated through parallel connections of different relaxation domains as follows:

$$1/E(T)=\sum_{i=1}^{n}\frac{\lambda_i}{\phi_f(z_i)E_{fi}+\phi_a(z_i)E_{ai}} \quad (\phi_f(z_i)+\phi_a(z_i)=1,\ \sum_{i=1}^{n}(\lambda_i)=1 \tag{26}$$

where λ_i is the fraction of each domain in the SMP, and $\phi_f(i)$ and $E_f(i)$ are determined by the equations (12) and (16), respectively.

Modeling results of equation (26) are plotted in Figure 6 and also compared with the DMA experimental data of MA-V/MP-A SMP reported in reference [16]. The values of fitting parameter are listed in Table 2. Clearly the MA-V/MP-A SMP shows a two-step transition behaviors, i.e., from 253 *K* to 302 *K* for the transition of MA-V component, and from 302 *K* to 362.3 *K* for the transition of MP-A component. Although the transition behaviors of these two-stages are different from each other, the transition behavior of the SMP is confirmed to be determined by the cooperative and collective dynamics of these two components. Therefore, the cooperative and collective model of equation (26) has been found to well predict the thermomechanical relaxation and transition behavior of the MA-V/MP-A SMP. The modeling results are in good agreements with the experimental data.

[Table 2]

[Figure 6]

According to equation (13), the changes of recovery strains were calculated and

then compared with the experimental data of MA-V/MP-A triple-SMP and EOC/LDPE/HDPE quadruple-SMP, reported in reference [16,17]. The results are shown in Figures 7(a) and 7(b), respectively. The values of parameters used for the simulations are listed in Table 3. As shown in Figure 7(a), there is a two-step strain recovery of the MA-V/MP-A triple-SMP. The first strain recovery occurs in the temperature range from 270 *K* to 301 *K*, which is originated from MA-V component transition. Whereas the second one occurs in the temperature range from 315 *K* to 344 *K*, which is originated from MA-V component transition.

On the other hand, the EOC/LDPE/HDPE quadruple-SMP presents a three-step strain recovery behavior, as shown in Figure 7(b). The SMP has its first strain recovery originated from the transition of EOC component. The second strain recovery is originated from the transition of LDPE component, and the third strain recovery is originated from transition of HDPE component. Furthermore, the modeling results fit well with the experimental data of the SMPs. It is verified that the proposed model is suitable to characterize and predict the strain recovery behavior of the SMP with multi-SMEs.

[Table 3]

[Figure 7]

4. Conclusion

In this study, an extended cooperative model is employed to identify the principle role of domain size in the collective dynamics of SMPs with multi-SMEs. It is found

that the multi-SME and multiple domain transitions can be achieved not only in the polymer with multiple domains, but also in the polymer with one domain which presents multiple domain transitions by means of programmed changes in temperature. The phase transition theory is then combined with multi-branch Maxwell model to describe the collective and cooperative relaxation behaviors of the amorphous SMPs. The modeling results using the proposed model have been plotted to compare with the experimental results of the storage modulus and strain recovery of SMP for verification. Results showed that the proposed model can well predict these experimental results. Finally, the domain size model is employed to characterize the multiple shape recovery behaviors of SMPs with triple- and quadruple-SMEs, respectively, and results showed the theoretical results fit well with the experimental ones. This study is expected to provide an effective approach to explore the working mechanism in multi-SME for the SMPs.

Acknowledgements

This work was financially supported by the National Natural Science Foundation of China (NSFC) under Grant No. 11672342 and 11725208, Newton Mobility Grant (IE161019) through Royal Society and NFSC.

References

[1] Liu C, Qin H and Mather P T 2007 Review of progress in shape-memory polymers *J. Mater. Chem.* **17** 1543–58

[2] Meng H and Li G 2013 A review of stimuli-responsive shape memory polymer composites *Polymer* **54** 2199–221

[3] Iv W S, Buckley P R, Wilson T S, Loge J M, Maitland K D and Maitland D J 2009 Fabrication and characterization of cylindrical light diffusers comprised of shape memory polymer *J. Biomed. Opt.* **13** 024018

[4] Lu H, Yao Y, Huang W M and Hui D 2014 Noncovalently functionalized carbon fiber by grafted self-assembled graphene oxide and the synergistic effect on polymeric shape memory nanocomposites *Compos. Part B Eng.* **67** 290–5

[5] Meng H, Mohamadian H, Stubblefield M, Jerro D, Ibekwe S, Pang S S and Li G 2013 Various shape memory effects of stimuli-responsive shape memory polymers *Smart Mater. Struct.* **22** 093001

[6] Teall O, Pilegis M, Davies R, Sweeney J, Jefferson T, Lark R and Gardner D 2018 A shape memory polymer concrete crack closure system activated by electrical current *Smart Mater. Struct.* **27** 075016

[7] Boyle A J, Weems A C, Hasan S M, Nash L D, Monroe M B B and Maitland D J 2016 Solvent stimulated actuation of polyurethane-based shape memory polymer foams using dimethyl sulfoxide and ethanol *Smart Mater. Struct.* **25** 075014

[8] Pilate F, Toncheva A, Dubois P and Raquez J M 2016 Shape-memory polymers for multiple applications in the materials world *Eur. Polym. J.* **80** 268–94

[9] Hu J, Zhu Y, Huang H and Lu J 2012 Recent advances in shape-memory polymers: Structure, mechanism, functionality, modeling and applications *Prog. Polym. Sci.* **37** 1720–63

[10] Lu H, Yu K, Liu Y and Leng J 2010 Sensing and actuating capabilities of a shape memory polymer composite integrated with hybrid filler *Smart Mater. Struct.* **19** 065014

[11] Santo L, Quadrini F, Accettura A and Villadei W 2014 Shape memory composites

for self-deployable structures in aerospace applications *Procedia Eng.* **88** 42–7

[12] Mao Y Q, Yu K, Isakov M S, Wu J T, Dunn M L and Qi H J 2015 Sequential self-folding structures by 3D printed digital shape memory polymers *Sci. Rep.* **5** 13616

[13] Liu Y, Du H, Liu L and Leng J 2014 Shape memory polymers and their composites in aerospace applications: A review *Smart Mater. Struct.* **23** 023001

[14] Feng X, Zhang G, Zhuo S, Jiang H, Shi J, Li F and Li H 2016 Dual responsive shape memory polymer/clay nanocomposites *Compos. Sci. Technol.* **129** 53–60

[15] Lu H, Wang X, Yao Y and Fu Y Q 2018 A "frozen volume" transition model and working mechanism for the shape memory effect in amorphous polymers *Smart Mater. Struct.* **27** 065023

[16] Chatani S, Wang C, Podgórski M and Bowman C N 2014 Triple shape memory materials incorporating two distinct polymer networks formed by selective thiol-Michael addition reactions *Macromolecules* **47** 4949–54

[17] Hoeher R, Raidt T, Krumm C, Meuris M, Katzenberg F and Tiller J C 2013 Tunable multiple-shape memory polyethylene blends *Macromol. Chem. Phys.* **214** 2725–32

[18] Xie T, Xiao X and Cheng Y T 2009 Revealing triple-shape memory effect by polymer bilayers *Macromol. Rapid Commun.* **30** 1823–7

[19] Xie T 2010 Tunable polymer multi-shape memory effect *Nature* **464** 267–70

[20] Yin T, Li Y and Yuan B Y 2018 The multi-scale flow behaviors of sisal fiber reinforced composites during resin transfer molding process *Science China Technological Sciences* **61** 1925–34

[21] Peterson G I, Childers E P, Li H, Dobrynin A V. and Becker M L 2017 Tunable Shape Memory Polymers from α-Amino Acid-Based Poly(ester urea)s *Macromolecules* **50** 4300–8

[22] Ge Q, Luo X, Iversen C B, Mather P T, Dunn M L and Qi H J 2013 Mechanisms of triple-shape polymeric composites due to dual thermal transitions *Soft Matter* **9** 2212–23

[23] Yu K, Dunn M L and Qi H J 2015 Digital manufacture of shape changing

components *Extreme Mechanics Letters* **4** 9–17

[24] Yu K, Ritchie A, Mao Y, Dunn M L and Qi H J 2015 Controlled Sequential Shape Changing Components by 3D Printing of Shape Memory Polymer Multimaterials *Procedia IUTAM* **12** 193–203

[25] Yu K, Xie T, Leng J, Ding Y and Qi H J 2012 Mechanisms of multi-shape memory effects and associated energy release in shape memory polymers *Soft Matter* **8** 5687–95

[26] Moon S, Cui F and Rao I J 2015 Constitutive modeling of the mechanics associated with triple shape memory polymers *Int. J. Eng. Sci.* **96** 86–110

[27] Lu H, Wang X, Xing Z and Fu Y Q 2019 A cooperative domain model for multiple phase transitions and complex conformational relaxations in polymers with shape memory effect *J. Phys. D. Appl. Phys.* **52** 245301

[28] Lu H, Wang X, Yu K, Fu Y Q and Leng J 2019 A thermodynamic model for tunable multi-shape memory effect and cooperative relaxation in amorphous polymers *Smart Mater. Struct.* **28** 025031

[29] Wang X, Lu H, Shi X, Yu K and Fu Y Q 2019 A thermomechanical model of multi-shape memory effect for amorphous polymer with tunable segment compositions *Compos. Part B Eng.* **160** 298–305

[30] Gibbs J H and Adam G 1965 On the Temperature Dependence of Cooperative Relaxation Properties in Glass-Forming Liquids *J. Chem. Phys.* **43** 139–46

[31] Matsuoka S 1997 Entropy, free volume, and cooperative relaxation *J. Res. Natl. Inst. Stand. Technol.* **102** 213

[32] Matsuoka S and Quan X 1991 A Model for Intermolecular Cooperativity in Conformational Relaxations near the Glass Transition *Macromolecules* **24** 2770–9

[33] Matsuoka S and Quan X 1991 Intermolecular cooperativity in dielectric and viscoelastic relaxation *J. Non. Cryst. Solids* **131** 293–301

[34] Liu Y, Gall K, Dunn M L, Greenberg A R and Diani J 2006 Thermomechanics of shape memory polymers: Uniaxial experiments and constitutive modeling *Int. J. Plast.* **22** 279–313

[35] Yang Q and Li G 2016 Temperature and rate dependent thermomechanical modeling of shape memory polymers with physics based phase evolution law *Int. J. Plast.* **80** 168–86

[36] Gupta P K and Mauro J C 2007 The laboratory glass transition *J. Chem. Phys.* **126** 224504

[37] Zwanzig R 2001 Nonequilibrium statistical mechanics, first ed Oxford University Press, Oxford.

[38] Arruda E M and Boyce M C 1993 Evolution of plastic anisotropy in amorphous polymers during finite straining *Int. J. Plast.* **9** 697–720

[39] Eldred L B, Baker W P and Palazotto A N 2008 Kelvin-Voigt versus fractional derivative model as constitutive relations for viscoelastic materials *AIAA J.* **33** 547–50

[40] Visintin A 2006 Homogenization of the nonlinear Kelvin-Voigt model of viscoelasticity and of the Prager model of plasticity Contin. Mech. *Thermodyn.* **18** 223–52

[41] Takayanagi M, Imada K and Kajiyama T 1967 Mechanical properties and fine structure of drawn polymers *J. Polym. Sci. C* **15** 263–81

Tables caption

Table 1. Values of parameters used in equation (13).

Table 2. Values of parameters used in equation (26).

Table 3. Values of parameters used in equation (13) to fit the strain recovery of EOC/LDPE/HDPE quadruple-SMP composite [17].

Figures caption

Figure 1. Schematic illustration of the viscoelastic behaviors of monomeric segments in Nafion SMP by means of the discrete domain size z_i.

Figure 2. Comparisons between the modeling results and experimental data [19] of the stored strain stress with respect to time. (a) A dual-SME by means of continuous heating method. (b) A multi-SME by means of segmental heating method.

Figure 3. Comparisons between the modeling results using equation (15) and experimental data [19] of the stored strains with respect to time.

Figure 4. Comparison between the modeling results of proposed model with the experimental data [19] of Nafion SMP with multi-SME.

Figure 5. A schematic illustration of relaxation behavior of SMP with multiple transition domains and their temperature-dependent phase transition behaviors.

Figure 6. Comparison of storage moduli of MA-V/MP-A SMP between the modeling results of equation (13) with the DMA experimental data [16].

Figure 7. (a). Comparison of strain recovery between the modeling results of equation (13) with the DMA experimental data [16] of MA-V/MP-A SMP. (b). Comparison of strain recovery between the modeling results of equation (13) with the DMA experimental data [17] of EOC/LDPE/HDPE quadruple-SMP.

Table 1.

	$\bar{z}$	z_1	z_2	z_3	z_4	z_5	$\Delta\mu\,(KJ/mol)$	$E_f\,(MPa)$	$E_a\,(MPa)$
$T_0(K)$	260	240	263	300	330	390	323.98	900	2.2
$\tau_0\,(min)$	3.72	1.12	2	2.2	2.4	2.5			
$q(K/min)$	4.5	4.0	4.0	4.0	4.0	4.0			

Table 2.

	T_0 (K)	τ_0 (min)	T_{ref} (K)	a	E_a (MPa)	ε_{pre} (%)
The 1st transition component	253	0.39	277	0.2	43.4	2.8
The 2nd transition component	303	0.11	314	$1.5\text{x}10^{-6}$	7.1	11.5

Table 3.

	T_0 (K)	τ_0 (min)	$\Delta\mu$ (KJ/mol)	ε_{pre} (%)
EOC component	290.12	2.11	1087.75	41.5
LDPE component	332.28	4.54	672.51	47.3
HDPE component	378	2.74	1032.43	11.2

Figure 1.

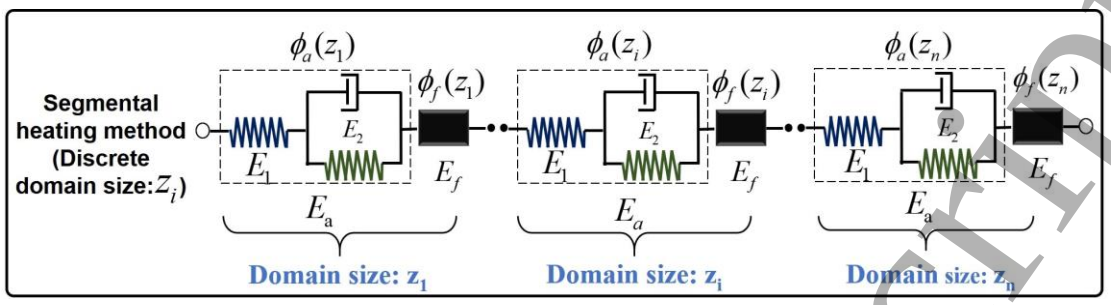

Figure 2.

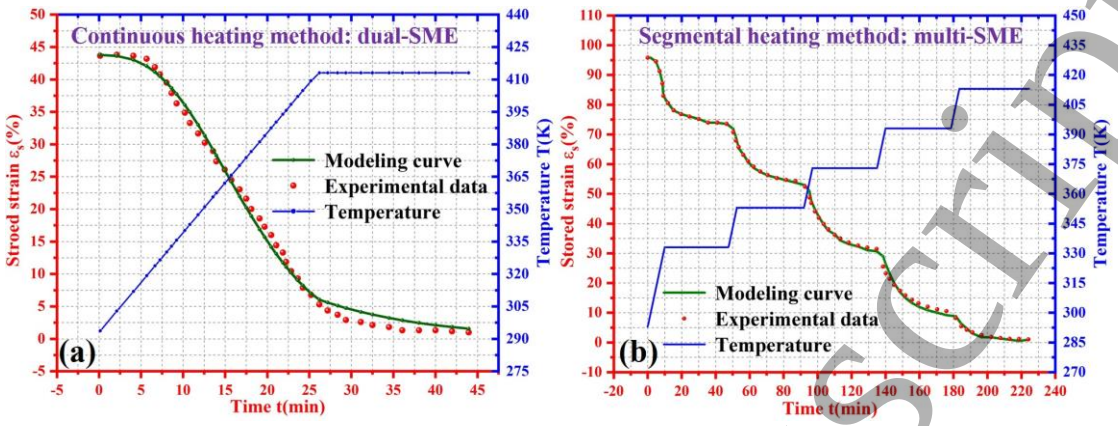

Figure 3.

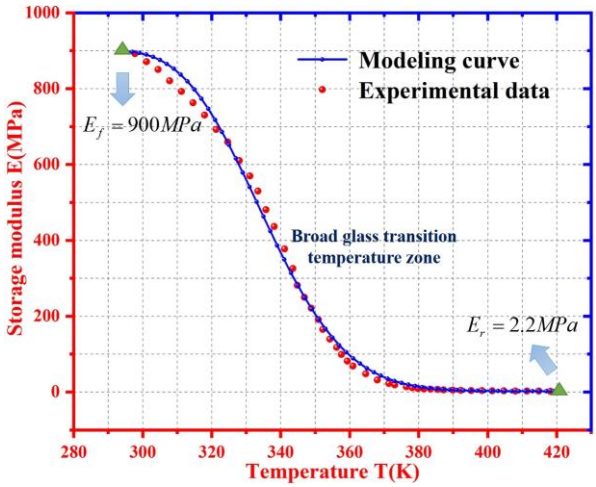

Figure 4.

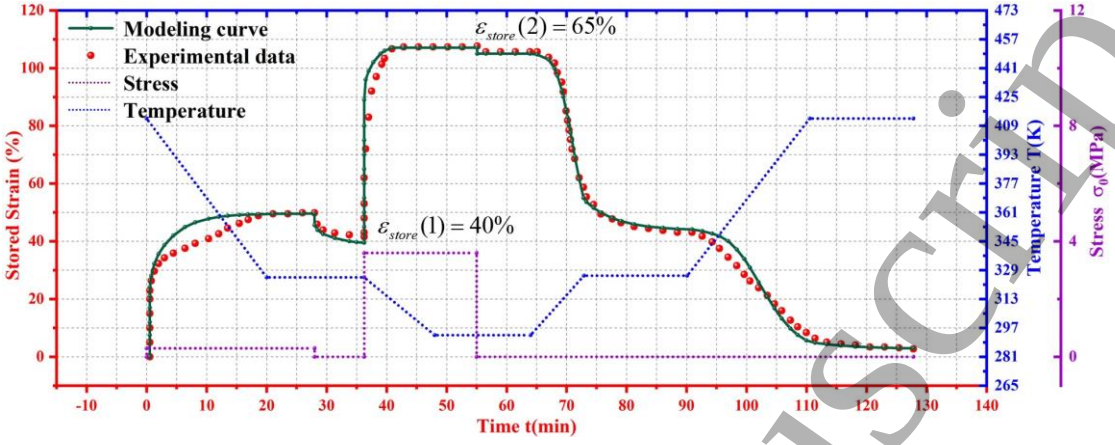

Figure 5.

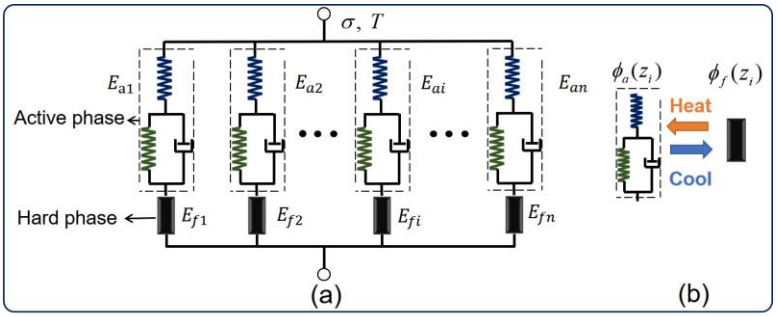

Figure 6.

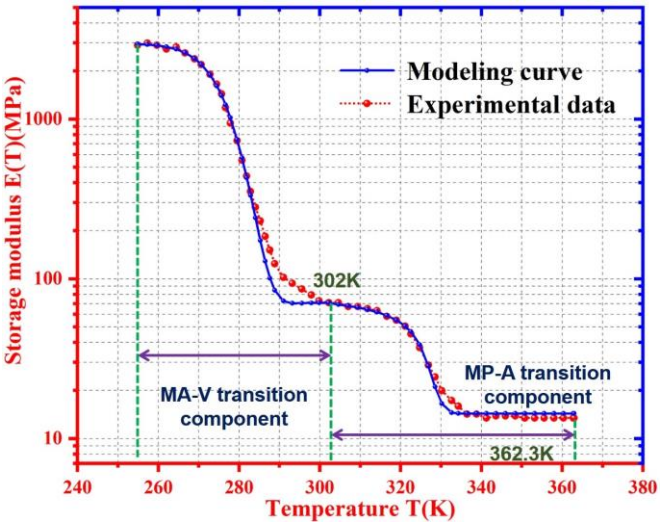

Figure 7.